

Vergleichende Visualisierung des Circulus arteriosus cerebri

BACHELORARBEIT

zur Erlangung des akademischen Grades

Bachelor of Science

im Rahmen des Studiums

Medizinische Informatik

eingereicht von

Hani Gadllah

Matrikelnummer 1128636

an der Fakultät für Informatik

der Technischen Universität Wien

Betreuung: Ao.Univ-Prof. Dipl.-Ing. Dr.techn. Meister Eduard Gröller

Mitwirkung: Dipl.-Ing. Haichao Miao

Wien, 9. Juni 2016

Hani Gadllah

Eduard Gröller

Comparative Visualization of the Circle of Willis

BACHELOR'S THESIS

submitted in partial fulfillment of the requirements for the degree of

Bachelor of Science

in

Medical Informatics

by

Hani Gadllah

Registration Number 1128636

to the Faculty of Informatics

at the TU Wien

Advisor: Ao.Univ-Prof. Dipl.-Ing. Dr.techn. Meister Eduard Gröller

Assistance: Dipl.-Ing. Haichao Miao

Vienna, 9th June, 2016

Hani Gadllah

Eduard Gröller

Erklärung zur Verfassung der Arbeit

Hani Gadllah
Am Schöpfwerk 29/14/27, 1120 Wien

Hiermit erkläre ich, dass ich diese Arbeit selbständig verfasst habe, dass ich die verwendeten Quellen und Hilfsmittel vollständig angegeben habe und dass ich die Stellen der Arbeit – einschließlich Tabellen, Karten und Abbildungen –, die anderen Werken oder dem Internet im Wortlaut oder dem Sinn nach entnommen sind, auf jeden Fall unter Angabe der Quelle als Entlehnung kenntlich gemacht habe.

Wien, 9. Juni 2016

Hani Gadllah

Acknowledgements

I would like to express my sincere gratitude to my advisor Haichao Miao for purposing this topic and for his continuous support.

Kurzfassung

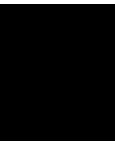
Das menschliche Gehirn wird von Arterien mit Blut versorgt, die einen Kollateralkreislauf, den sogenannten Circulus arteriosus cerebri, bilden. Die Anatomie dieses Arterienrings variiert in der Bevölkerung sehr stark. Tatsächlich findet sich der im Lehrbuch skizzierte Circulus arteriosus cerebri je nach Studie nur bei 13% bis 72% der Bevölkerung. Abweichende Konfigurationen sind in der Regel zwar nicht pathologisch, doch erhöhen einige Konfigurationen mit einem inkompletten Arterienring das Risiko für einen Schlaganfall. Auch zeigen einige Studien einen möglichen Zusammenhang zwischen bestimmten neurologischen Erkrankungen und anormale Formen des Arterienrings. Zur Diagnose und Behandlung diverser Krankheiten spielt die Beurteilung des Arterienrings des Patienten daher eine wichtige Rolle. Die vorliegende Arbeit beschäftigt sich mit der Entwicklung einer Software zur vergleichenden Visualisierung der Arterienringe einer Population mit den Arterienringen einer zweiten Population. Hierfür wird für die beiden Populationen jeweils ein durchschnittlicher Arterienring berechnet. Die beiden resultierenden Arterienringe werden dann anschließend nebeneinander visualisiert, so dass der Betrachter Unterschiede zwischen den Arterienringen der beiden Populationen mit relativ wenig Aufwand finden kann. Das Ziel dieser Visualisierung ist zum einen die Unterstützung von Studien, die sich mit der klinischen Bedeutung der unterschiedlichen Konfigurationen des Arterienrings befassen. Zum anderen soll die Software eine Unterstützung bieten bei der Diagnose und bei der Behandlung von Krankheiten die durch eine anormale Konfiguration des Arterienrings verursacht wurden. Letzteres kann dadurch erreicht werden, indem der Arterienring des Patienten mit den Datensätzen von Risikogruppen oder dem Datensatz einer gesunden Population verglichen wird.

Abstract

The human brain is supplied with blood by arteries that form a collateral circulation, the so-called Circle of Willis (CoW). The anatomy of the CoW varies considerably among the population. In fact, depending on the study, just 13% to 72% of the population does have the typical textbook illustration of the CoW. Although divergent configurations are usually not pathological, some incomplete configurations increase the risk of stroke. Furthermore, studies suggest an association between certain neurological diseases and abnormal configurations of the CoW. Thus, for the diagnosis and treatment of diverse neurological diseases the assessment of the patient's CoW is an important issue. This thesis addresses the development of a software for a comparative visualization of the CoWs of a population with the CoWs of a second population. For this purpose, an average CoW is calculated for each of the populations. The two resulting CoWs are then visualized side-by-side, so that the viewer is able to distinguish differences between the CoWs of the two populations with relatively little effort. The aim of this visualization is the support of studies that consider the clinical significance of the different CoW configurations as well as the support of diagnosis and treatment of diseases that are caused by an abnormal configuration of the CoW. The latter can be achieved by comparing the patient's CoW with datasets of risk groups or with a dataset of a healthy population.

Contents

Kurzfassung	ix
Abstract	xi
Contents	xiii
1 Introduction	1
1.1 Motivation	1
1.2 Circle of Willis	2
1.3 Data Visualization	6
2 Releated Work	9
2.1 Comparative Visualization Designs	9
2.2 Comparative Visualization of Trees	12
2.3 Circle of Willis Visualization as Radial Graph	12
3 Methodology	17
3.1 Implementation	17
3.2 Visualization of the Spatial Information	18
3.3 Visualization of the Quantitative Attributes	21
3.4 Data Acquisition	29
3.5 User Interaction	31
4 Future Work and Discussion	33
List of Figures	35
List of Tables	35
Bibliography	37



Introduction

1.1 Motivation

Medical imaging, such as radiography, magnetic resonance imaging and computed tomography are indispensable in both, medical diagnosis and research as they allow to look inside a human body without an exploratory surgery. The so-called magnetic resonance angiography (MRA) enables to acquire images of the brain's vessel structure. By evaluating these images, a radiologist can detect anomalies of the patient's brain vessels, e.g. to find a location that cause a stroke or to evaluate the risk of a patient to suffer a stroke. However, the images that are acquired from the MRA are even for experienced radiologists tedious to read (see Figure 1.1). For this reason, it is reasonable to use visualization techniques to map MRA images into an easy to read image. This does not mean that the resulted visualization should look like the real vessel structure. Three-dimensional images have the disadvantage, that the entire image cannot be seen at once. The user have to rotate the image to see it from different angles, which is why a comparison of three-dimensional images requires more mental effort from the user than a comparison of two-dimensional images. Apart from this, an abstract visualization can highlight characteristics, such as the diameter of the vessel better than the visualization of the real vessel structure. Additionally, abstraction enables to compare a certain vessel structure of a population with the vessel structure of a second population or with the vessel structure of a patient. The former is useful for studies while the latter can support radiologists by detecting anomalies or a specific risk profile. In general, abstract visualization simplifies the appearance of real objects and draws attention to important characteristics. A visualization that compares characteristics, such as length and diameter can of course be replaced by tables. However, in comparison to a proper visualization, tables are not that comfortable to read. Parsaye and Chignell [22] wrote in this regard: *"To see and understand pictures is one of the natural instincts of human, and to understand numerical data is a years skill from school, and even so, a lot of people*

are still not good with numerical data." Hence, in this thesis an abstract visualization will be implemented that enables both, the comparison of the most important brain vessels of two populations and the comparison of the vessel structure of a population with the vessel structure of a patient. The implemented visualization can be theoretically used for studies and diagnostic purposes, although for the latter at least a big dataset of vessel data is needed.

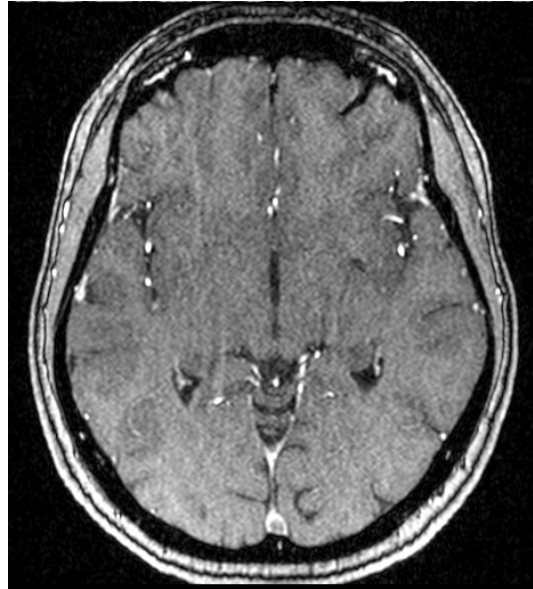


Figure 1.1 – MRA slice of the brain’s vessels. High intensity values represent the vessels. To get the entire picture of the vessels, a radiologist has to analyze each of the slices by following the pathway of the high intensity values across the slices. Image courtesy of Miao et al. [20].

1.2 Circle of Willis

1.2.1 Anatomy

The Circle of Willis (CoW, see Figure 1.2) is a circulatory system that enables the blood supply of the brain. It is located in the base of the brain, whereas the origin is formed by four big arteries. Two of them are the left and right common carotid artery. They split each into an internal carotid artery (ICA) and an external carotid artery. The end of the former marks the beginning of the left anterior and right anterior part of the CoW respectively. The other two big arteries are the left and right vertebral artery. They extend the subclavian arteries and merge to the basilar artery (BA) that is the main artery of the posterior part of the CoW. The two ICAs and the BA are connected through further branches to build a circle of blood circulation, i.e. a circulatory anastomosis. However, the connections are not always strong enough to compensate a constricted part, as the radius of the arteries that connect the three parts, i.e. the communicating arteries,

the posterior communicating artery (PCoA) arises and terminates by branching into the middle cerebral artery (MCA) and the anterior cerebral artery (ACA). The MCA has four segments (M1-M4). Although none of these segments are a part of the CoW, the M1 segment can be a site of ischemic stroke and thus has a clinical significance. Therefore it will be considered as part of the CoW. The ACA has three segments (A1-A3), where the first segment is a connection between the anterior communicating artery (ACoA) and the ICA. Thus the ACoA connects the left anterior part with the right anterior part. Only the first segment of the ACA is a part of the CoW. However, since there are common variations of the ACA's A2 segment that are discussed in the literature, the latter will be considered as part of the CoW. The BA bifurcates into the left and right posterior cerebral artery (PCA). These arteries have four segments (P1-P4), whereas only the P1 segment is a part of the CoW. The left and right P1 segments are connected with the left and right PCoA respectively. Thus the PCoAs connect the posterior part of the CoW with the left and right anterior part.

1.2.2 Configurations

There are a huge number of studies that examined the configurations of the CoW. According to these studies the incidence of the standard CoW as shown in Figure 1.2 ranges from 13% to 72% [15]. This wide range can be explained by three reasons. The first one is the different subject groups of the studies, e.g. some studies exclude people with cerebrovascular disorders to investigate the variations of a healthy population while other studies focus on an unhealthy population. Second, the method that is used for the data acquisition has a significant effect on the study results, e.g. autopsy studies tend to have a higher incidence of a standard CoW [9]. The third reason is that there are different criteria for considering a CoW as standard. For example, in some studies a CoW is considered as complete if the ACoA is missing and the left and the right ACAs are joined together while other studies always consider the CoW as incomplete if the ACoA is missing [15].

The configurations are formed mainly by absent, hypoplastic, duplicated and triplicated segments as well as by the persistence of the embryonic patterns [15]. Chen et al. [9] examined the CoW of 507 subjects and classified the observed configurations in ten patterns for the anterior part and ten patterns for the posterior part of the CoW (see Figure 1.3). Klimek-Piotrowska et al. [16] examined the CoW of 250 subjects by using a similar classification system as the one used by Chen et al. However, in the anterior part, ten (4%) findings had a configuration that could not be described by a pattern from the used classification system (see Figure 1.4). Since all of these ten findings have a different configuration, it is safe to assume that they are outlier.

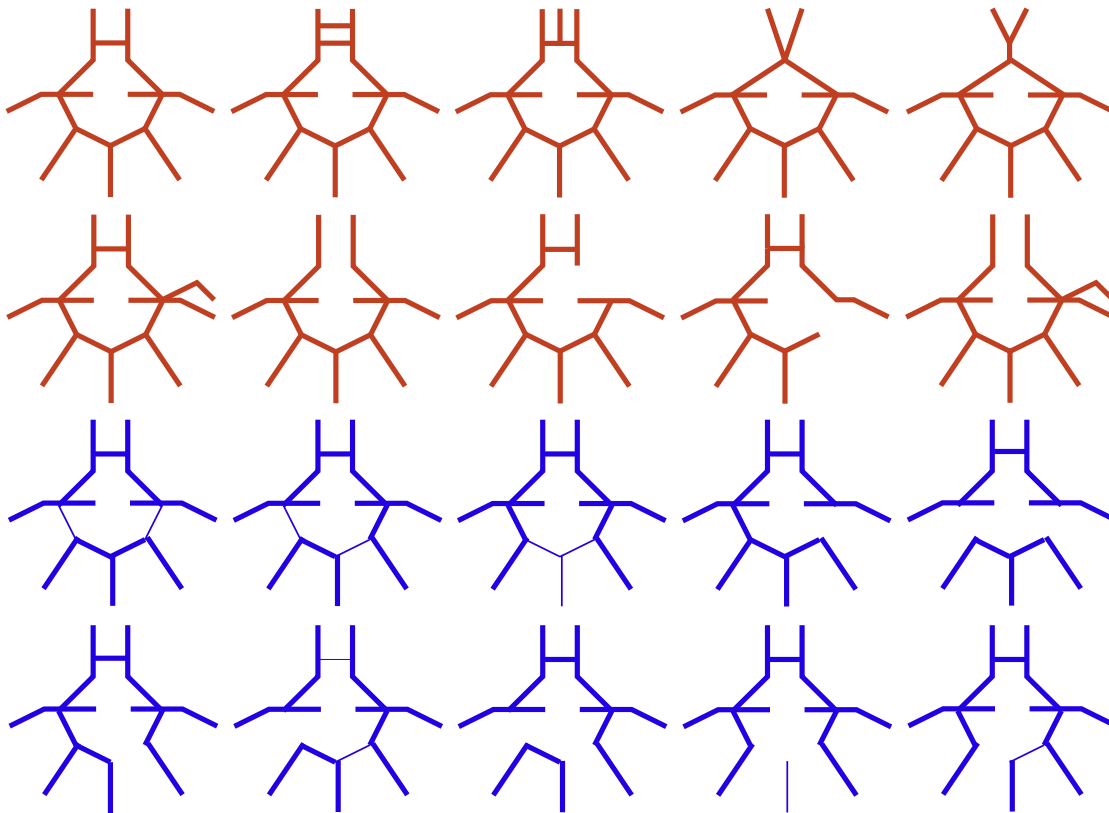


Figure 1.3 – Schematic diagrams of anatomic variations in the anterior part (red) and in the posterior part (blue) of the CoW [9].

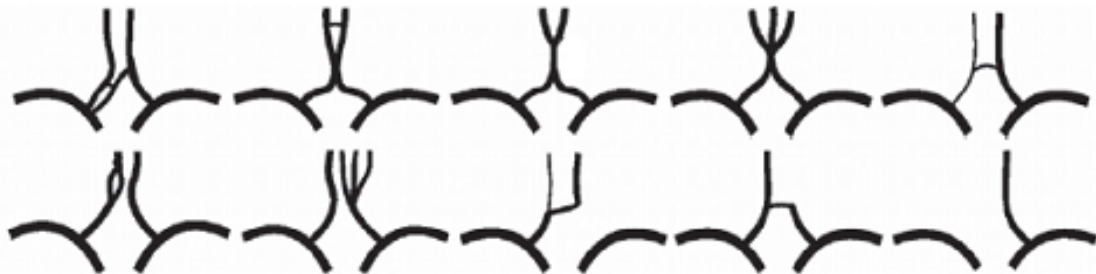


Figure 1.4 – Ten unclassified variants of the anterior part of the CoW. Figure taken from [16].

1.2.3 Pathology

Although the variety of the CoW configurations has been extensively studied, the functional and clinical implications have been investigated just by a few studies. Cucchiara et al. [10] conduct a study regarding the relation between an incomplete CoW and migraine. Due to the limited sample size the association between migraine and the

different configurations of the CoW could not be analyzed. However, it turned out that an incomplete CoW was significantly more common in the so-called migraine with aura group, i.e. a type of migraine headache with additional neurological symptoms. A study from Beach et al. [4] have found a statistical association between intracranial atherosclerosis and Alzheimer's disease. Intracranial atherosclerosis is the narrowing and hardening of the vessels inside the brain, i.e. the vessels of the CoW. The narrowing leads to a slowed blood flow, which does not only increases the risk of an undersupply of the affected brain tissue and thus of an ischemic stroke, but it leads also to a higher blood pressure at the affected site. As atherosclerosis leads to an increased arterial stiffness, it increases the risk of a vessel rupture, which causes a hemorrhagic stroke. Besides of atherosclerosis, there are other risk factors for stroke such as thromboses, embolisms and traumas. Stroke is the second most common cause of death [1], whereas the most strokes are ischemic. van Seeters et al. [23] have found that an incomplete anterior part of the CoW is related to an anterior circulation stroke (i.e. an ischemic stroke in the anterior part). While no relation was found between an incomplete posterior part of the CoW and an anterior circulation stroke, it was found that people with both, an incomplete anterior part and an incomplete posterior part, have the highest risk of an anterior circulation stroke. The study of van Seeters et al. is an example of the importance of the CoW configurations in a clinical context, as knowing as much risk factors as possible is the best way to avoid a stroke.

1.3 Data Visualization

1.3.1 Motivation

Data visualization is about enabling an effective comparison of information as well as an effective search for relations and patterns within this information by presenting the information graphically in an intuitive way, so that we can interpret them with as little cognitive effort as possible. The visual comparison of information is referred to as comparative visualization. An example for information are the three real numbers 797.67, 265.89 and 88.63. This numerical sequence has a certain pattern that we can't see by just looking at the numbers. It takes some time and cognitive work to figure out the pattern. However, a visualization of the numbers reveals the pattern immediately (see Figure 1.5). Pearson's correlation coefficient r is a measure of the linear association between a sample of entities with two features, e.g. the bodyweight and height of people. A complete linear association has a value of 1 or -1, whereas the linear association is weaker the lower $|0 - r|$ is. Visually each entity can be interpreted as a point in a Cartesian coordinate system where the points form a shape. The more similar the shape is to a line, the stronger the linear correlation is. If the points form a circle, r would be zero, indicating that there is no relation between the features while the visualization would show a perfect deterministic relation. As this example shows, data visualization can reveal information as a visualization always tells more than just a number or numbers. In the following, a brief introduction of the most important visualization principles will be given. The

choice of the principles based on [21].



Figure 1.5 – Visualization of the number sequence 797.67, 265.89 and 88.63.

1.3.2 Attribute Types

Data can be seen as a table where the rows are referred to as items and the columns as attributes. The latter can be roughly classified in three types: quantitative, ordered and categorical. Quantitative attributes are numerical and have either an interval scale, where differences are interpretable but statements such as "half as late" or "twice as hot" are not, or a ratio scale where differences as well as multiplications and divisions have a meaning. Examples for the latter are the length or diameter of a vessel. Ordered data, such as the clinical significance of a vessel segment, have a well-defined order as the only relation, so that logical operations are possible while mathematical are not. Categorical data are just classifications of features, e.g. the classification of the CoW segments in an anterior and a posterior part can be seen as categorical. Items are rational if they can be modeled as a graph with nodes and edges. This is true for the CoW segments, as each segment is connected to at least another segment. In addition items are either spatial, e.g. the location of a vessel segment, or non-spatial.

It is not always the best idea to use the original types of the attributes for the visualization. A more effective approach is to adapt them to the specific needs of the target audience or task by changing their types. For example, in a comparison of anthropometric data between two populations, it may not be of interest whether a specific attribute, e.g. the bodyweight, differs by two or five percent but rather if the difference is statistically significant. In this case the anthropometric attributes would be transferred from a quantitative to a categorical type with far less distinguishable values.

1.3.3 Visual Channels

Attribute types can be visualized by different visual channels, such as length, color, shape and area. There are three considerations to take into account when choosing a visual channel. First, the viewer should be able to identify even small distinctions with minimal cognitive effort. Studies have found that the discriminability does not only depend on the visual channel but also on the attribute type (see Figure 1.1)[21]. Second, the visual channels for different attributes have to be separable. For example, color and length

are separable while shape and area are not that easy to separate. Third, an unexpected value of a visual channel, e.g. a green circle among white circles, leads to a popup effect.

Quantitative	Ordered	Categorical
Position	Position	Position
Length	Lightness	Hue
Angle	Saturation	Texture
Slope	Hue	Connection
Area	Texture	Containment
Volume	Connection	Lightness
Lightness	Containment	Saturation
Saturation	Length	Shape
Hue	Angle	Length
Texture	Slope	Angle
Connection	Area	Slope
Containment	Volume	Area
Shape	Shape	Volume

Table 1.1 – Effectiveness of visual channels depending on the attribute type [21].

The color channel is subdivided into the three channels hue, lightness and saturation. Tamara Munzner [21] recommends to use high saturated colors for small areas and low saturated pastel colors for big areas. This is because in small areas colors are difficult to perceive while in big areas high saturated colors are hard to view. For a few categorical attribute values hue is an effective visual channel. However, hue should not be used if more than seven colors are needed as people cannot distinguish more colors reliably[21]. Lightness and saturation are effective channels for ordered attributes as they have a gradient from the low to the high value but they are unsuitable as categorical attributes. For example, data that show different age groups of males and females have a categorical attribute (sex) and an ordered attribute (age group). While the former can be coded with a blue hue for male and a red hue for female, the age groups can be coded with the saturation channel, whereas a lower saturation means a lower age group.

1.3.4 Limitations and User Interaction

Sometimes the desired information is too much to be visualized in a single screen. The limited display size is not the only reason for being unable to display all the desired information at once, as the limited human perceptual resources have to be taken into account as well. To tackle this issue, the visualization can be designed interactive. While interactivity can be powerful, it should not be overused, as the more interaction a visualization requires from the user to reveal all the information, the more time and attention will be required from the user.

Related Work

For choosing a proper solution that visually compares two specific objects, it is helpful to understand the basic principles as well as common challenges of comparative visualization in general, i.e. independent of the compared objects [11]. For this reason, in this section an overview of comparative visualization designs will be given, although some approaches are not directly related to a comparative visualization of vessel structures. In the second part, approaches that can be adapted to the specific needs of the CoW visualization will be discussed. Miao et al. [20] purposes an abstract visualization of the CoW that in theory enables an abstract comparison of two or more CoWs. This purpose will be described in the third part. However, Miao et al. [20] do not focus on a comparative visualization of the CoW. To the best of our knowledge, a comparative visualization of the CoW has not been attempted before.

2.1 Comparative Visualization Designs

Gleicher et al. [11] conduct a survey of comparative data visualization literature where they analyzed 173 designs. Based on that, they classified the designs in six categories, whereas three of them are basic categories, namely juxtaposition, superposition and explicit encoding. The other three are hybrids of the basic categories. In this section the basic categories will be discussed.

2.1.1 Juxtaposition

A comparative visualization that shows the objects to be compared independently next to each other is classified as a juxtaposition design [11]. Although it is relatively easy to implement, as only independent objects have to be visualized, this approach has two drawbacks. The first one is that with each object that is displayed for the comparison, the available display size for the individual objects shrinks. The second one is that this design

requires memory capacity from the user, as the user has to memorize the appearance of the objects to be able to compare them. Therefore, juxtaposition designs do not scale well and are not intuitive as well. To address this issues, juxtaposition designs are in most cases designed interactive, which often leads to a hybrid design.

An example for a visualization strategy that has to deal with the limited display space as well as the limited cognitive human resources is Cerebral [3]. This is a software for visualizing biological systems (e.g. proteins and gens), i.e. the behavior of, in case of Cerebral, up to 3000 biological entities that influence each other under specific experimental conditions (e.g. the introduction of a drug or the change in environmental temperature). The biological entities are visually encoded as nodes and the interaction between them as edges. Thus a visualization of a biological system forms a graph. The nodes are colored according to the their expression level. Cerebral is able to visualize a few dozen graphs on the display, whereas each graph has a different experimental condition, i.e. the same shape but different colored nodes. As it is impossible to show a few dozen detailed graphs with 3000 nodes each, in Cerebral the user can select one of the graphs that is displayed as a big graph in more detail while the other graphs are displayed in small boxes (see Figure 2.1). Barsky et al. [3] considered two other strategies to deal with the limited display size. The first is to change the colors of the nodes over time to show the different experimental conditions with just one graph. However, while this would increase the available display size, more memory work would be needed from the user to compare the graphs. The second is to visually encode the different experimental conditions within the nodes of a single graph. But since a graph has up to 3000 nodes, the nodes can become too small to carry more than just one attribute. To address the difficulty of comparing that much nodes, Cerebral helps the user to find areas that are worth to explore with various techniques. For example, to facilitate finding outliers a third view is displayed that visually encodes each experimental condition as a parallel axis in a coordinate system and the biological entities as lines. While lines with normal values have a similar pathway and thus merge to a thick line, outliers have different pathways, which is why they stand out (see Figure 2.1). This view is called parallel coordinates view.

2.1.2 Superposition

A design that shows the objects to be compared in the same space is classified as a superposition design [11]. As example, the parallel coordinates view of Cerebral (see Figure 2.1) has a superposition design as the biological entities are visually encoded as lines in the same space. While the strong merging effect of Cerebral's parallel coordinates view is a desired effect, this is not always the case. In some cases a strong merging effect harms the clarity. For example, to compare two images with a superposition design, one image can be overlaid over the other, whereas the former is semi-transparent. However, overlaying a third or a forth image would lead to an unclear visualization. Thus, depending on the comparative visualization task, techniques has to be used to avoid merging effects. Malik et al. [18] tackled this issue by using hexagons that are divided

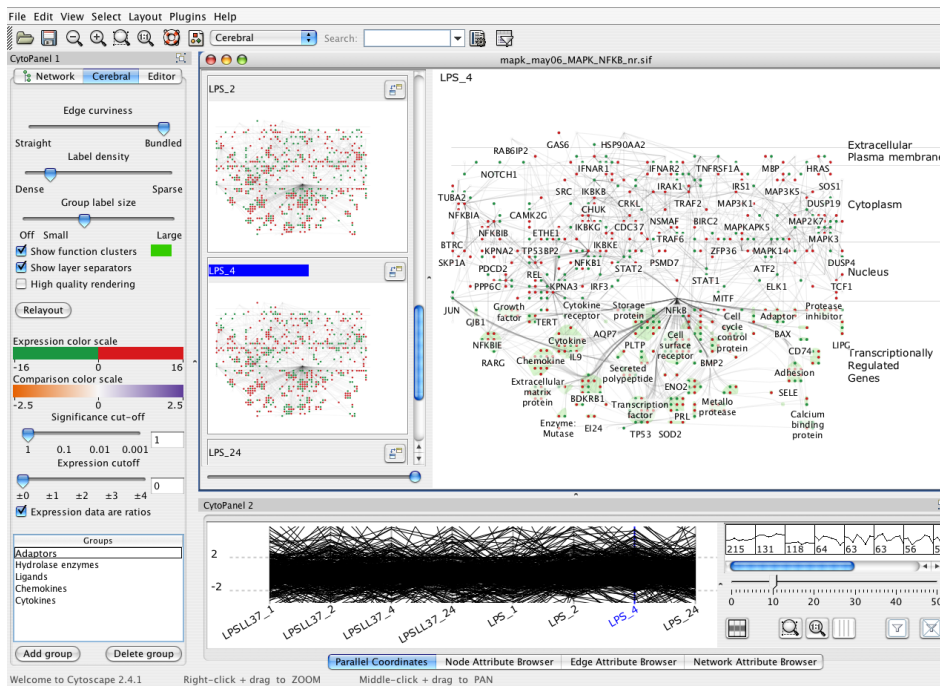


Figure 2.1 – User interface of the visualization software Cerebral. Figure taken from [3]

into multiple sectors. Each sector carry an attribute value of a different dataset, where the hexagons form a grid over the space. This approach can be adapted for visually encoding and displaying more than two samples of the CoW at once. However, because of the limited display size, it would be difficult to show more than just one attribute while retaining an intuitive shape of the CoW.

2.1.3 Explicit Encoding

An explicit encoding design focuses on the relationships between the objects to be compared [11]. This is achieved by visually encoding the objects as a single object that shows the relationships. Cerebral [3] enables to display a graph that visualizes the difference of two experimental conditions. This is a typical example for an explicit encoding design, which can also be used for a comparative CoW visualization as differences e.g. in diameter are from high interest. In contrast to juxtaposition and superposition, explicit encoding relies on the knowledge of which relationships are from interest as well as algorithms that are able to compute the relationships. An example for issues of the latter is Mizbee [19]. This is a visualization for comparative genomics, i.e. the comparison of genomes of different species. Mizbee compares automatically the similarity of gene sequences (i.e. parts of genomic) and visually encodes the relationships by color encoding and edges. However, the results of the visualization depend on parameters that are chosen from the user and can thus be unreliable if the parameters are not chosen properly. This limitation of explicit encoding has to be taken into account when choosing a design

category. Visualization of vessel structures can encounter this issue of an unreliable algorithm, if the software includes the segmentation algorithm that acquire the data from the images of the medical imaging device [20]. Since data acquisition is not a part of this thesis, it is assumed that the visualization software works with reliable data. Hence, in this thesis explicit encoding can be used without this limitation.

2.2 Comparative Visualization of Trees

Vessel structures can be visualized as a graph that form a tree or, e.g. in case of the CoW, as a graph that can be seen as connected trees, where edges visualize the connections between the segments and segments are represented by nodes. Therefore, the visual comparison of trees is closely related to the comparative visualization of vessel structures. Guerra-Gomez et al. [12] developed an application for comparing the topology as well as the node values of two trees. Their approach based on a so-called icicle plot [17]. This is a tree-like structure where the levels of the hierarchy are visualized as horizontal rows with an equal length. The rows are divided with vertical lines so that each node is represented as a box. Guerra-Gomez et al. changed the icicle plot by adding a horizontal line in the center of the rows that represents a zero value of an attribute. A difference of an attribute is then visualized as a bar that starts at this horizontal line and goes to the top if the difference is positive and to the bottom if the difference is negative, whereas the height and the color of the bars encodes the relative or absolute value of the attribute. A missing node is visualized by a white border of the box and an additional node by a black border. This visualization is called StemView (see Figure 2.2).

The StemView can be adapted to the specific needs of the comparative CoW visualization. This can be achieved by encoding each part of the CoW as a StemView where the ICAs and the BA form the roots. By placing the StemView of the left anterior and right anterior part on the left and right of the display respectively and the posterior part on the bottom of the display, the spatial information can be partly visually encoded. Each StemView can be bordered with a color that represents the CoW part, e.g. a red color hue for the left anterior part, a green for the right anterior part and a blue for the posterior part. To show the connections between the parts, small circles with the color of the corresponding part can be placed on the top of the boxes (i.e. segments) where the parts are connected. Instead of one bar two or three bars can be used to visualize more than just one attribute. While this approach might work well for the comparative CoW visualization, in this thesis a more intuitive visualization will be implemented that shows the spatial information immediately.

2.3 Circle of Willis Visualization as Radial Graph

Another approach that is inspired from the tree-like structure is purposed by Miao et al. [20]. They visualized the CoW as radial graph where each part of the CoW is modeled as a tree. The root of the trees are the two ICAs for the left and right anterior tree and the

2.3. Circle of Willis Visualization as Radial Graph

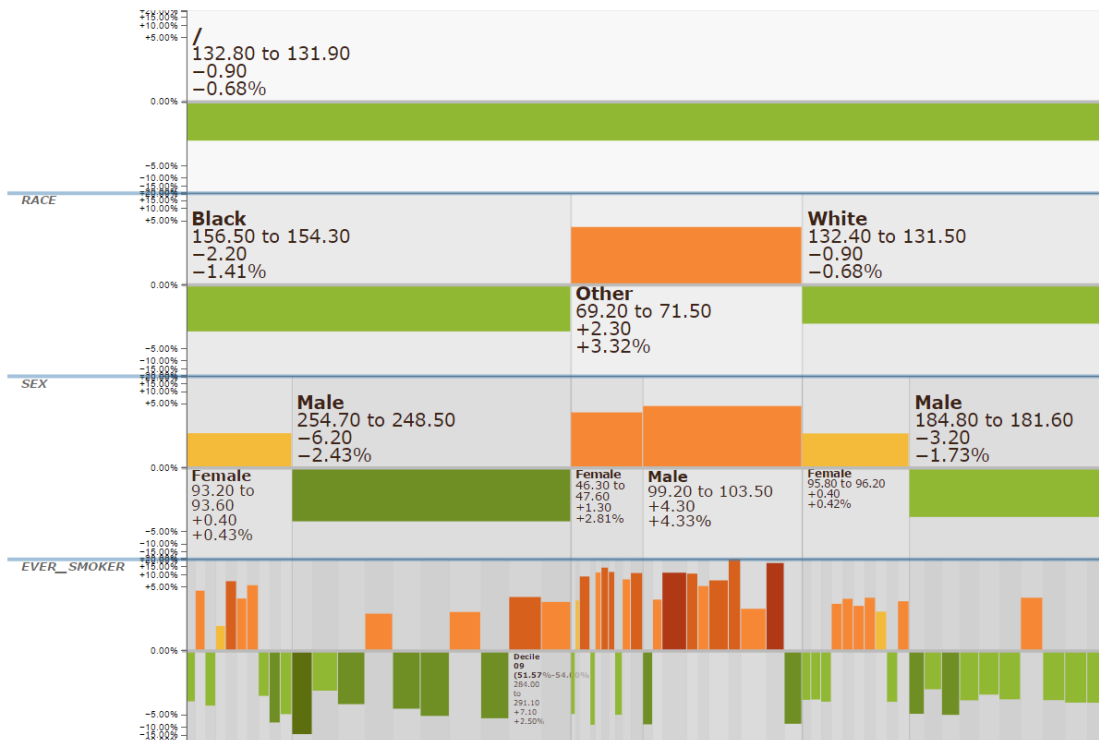


Figure 2.2 – StemView that shows the related death-rate change of Lung Cancer between 1999 and 2000 in the US.

BA for the posterior tree. In case of a connection between two trees, e.g. a connection between the left and right anterior part formed by an ACoA, the affected leaves of the two trees will be connected with the vessel segment that connects them. The latter is considered as a part of the left anterior, right anterior or posterior tree, depending on its location. Attributes of the vessels are visually encoded as bars in the nodes. Miao et al. [20] referred this visualization to as Circle of Willis Radar (CoWRadar). Figure 2.3 shows a CoWRadar of a stroke patient. The connection between the left and right anterior tree indicates that this parts are connected and thus suggests the existence of the ACoA, while the missing connections between the anterior trees and the posterior tree suggest the absence or a hypoplasia of the PCoAs.

As it can be seen in Figure 2.3, the segments are not referred to by their anatomical names. Instead, the segments are labeled systematically according to the following rules: Each label starts with one of the three letters L, R and B, which refer to the root of the tree. L and R refers to the left and right anterior tree respectively and B to the posterior tree. The letter is followed by a number that represents the number of edges between the root of the tree and the segment of the label. The third character is a lowercase that represents the branching number from the parent node, e.g. a node that bifurcates has two child nodes where one has the branching number one mapped as "a" and the other

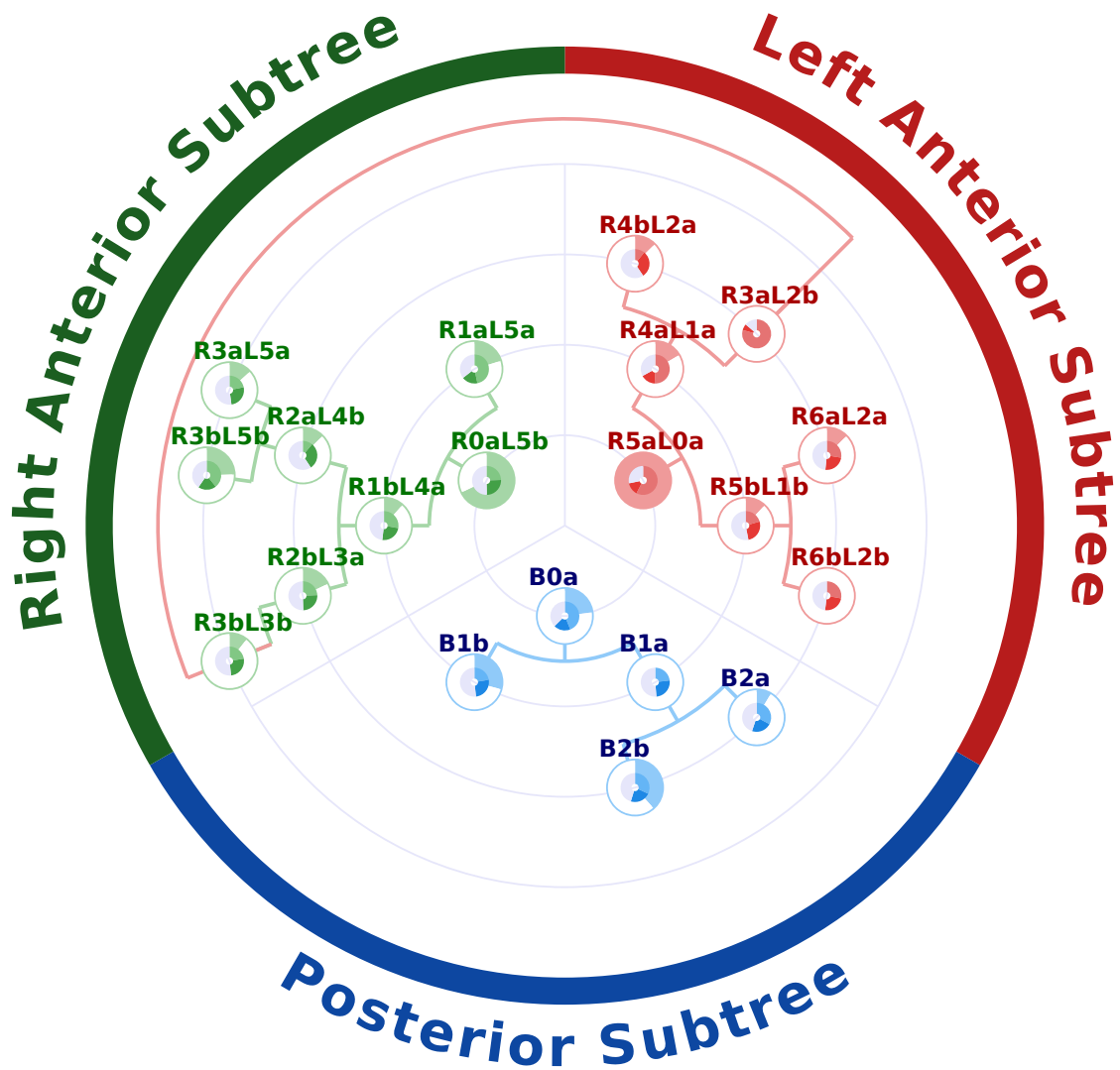


Figure 2.3 – Circle of Willis Radar. The nodes visually encode the vessel segments and the edges visually encode the connections between the segments. Bars are used in the nodes to visually encode attributes of the vessel segments.

the branching number two mapped as "b". Each node has such a label for each tree that has a connection to the node, e.g. R1aL5a means that the segment is connected with the left and right anterior tree but not with the posterior tree. Although this labeling system is easy to understand, radiologists are familiar with the anatomical names. Hence, the described labeling system aggravates the interpretation of the visualization. One of the reasons why this labeling system was chosen is because Miao et al. [20] not only purposed a visualization of the CoW but they also developed a pipeline that acquires the needed data for the visualization automatically from TOF-MRA images. As an algorithm for anatomical labeling of vessels is an own research field, an alternative labeling system was

developed. In general, the CoWRadar is a bit too abstract. This is not only true for the labeling system but also for the visualization as a whole. Radiologists are not used to work with graphs where the segments are visualized as nodes but they are familiar with schematic illustrations of the CoW like the illustration in Figure 1.2.

Methodology

This chapter first introduces the used visualization framework. Then the design choices of the implemented visualization will be discussed in four subsections: the visualization of the spatial information, the visualization of the quantitative attributes, the data acquisition and the user interaction. The design choices are based on results from the literature regarding human cognitive and visual perception and are inspired by other comparative visualization tools (see Section 1.3 and Section 2).

3.1 Implementation

The visualization is implemented in JavaScript using the visualization framework Data-Driven-Documents (D3.js) [6]. JavaScript was chosen because it enables to run the visualization software with any common browser straightforward and independent from the used operating system. D3.js was developed by Bostock et al. [6] as the successor of the popular visualization framework Protovis, which was released in 2009. The popularity of Protovis was based on its accessibility. This was achieved by an intermediate abstraction layer, i.e. an abstraction of the more complex underlying layer that is developed with simplification in mind. For example, to visualize a bar in Protovis the following code can be used:

```
svg.add(pv.Bar)
    .left(0)
    .top(0)
    .width(100)
    .height(10);
```

This bar is visualized as a scalable vector graphic (SVG), but the user of Protovis does not need to know anything about SVGs to visualize the bar. This is the result of the intermediate abstraction layer that hides low-level details. However, this simplification is

a trade-off as it lowers the performance, limits the expressiveness, leads to a scarcity of documentation and makes debugging more difficult. These drawbacks were concluded by Bostock et al. [6] after they evaluated the observations of thousands of users during two years. To tackle this issues they developed D3.js and released it in 2011 as the successor of Protovis. D3.js uses a low-level approach. It works with existing technologies such as HTML, CSS and SVG by enabling the developer to manipulate them directly. For example, a bar can be visualized by using the following code:

```
.attr("x", 0)
.attr("y", 0)
.attr("width", 100)
.attr("height", 10);
```

Like Protovis, this bar is visualized as a SVG. However, in this approach the user manipulates the SVG directly. Thus, the user has to know about the SVG standard. This leads to a steeper learning curve, at least for users which are not familiar with the used standards, and to a more complex code for equal tasks that are written with Protovis. However, in exchange this approach improves the performance, the expressiveness, the debugging and the documentation support.

3.2 Visualization of the Spatial Information

The objective of this thesis is to purpose a comparative visualization of the CoW where the shape of the CoW is as intuitive as possible. The user should be able to identify all of the segments immediately. For this reason, the CoW will be not visualized as a graph. Graphs have admittedly the advantage of scalability as they are not only able to visualize any imaginable variation of the CoW, but they also can be adapted to visually encode other vessel structures with little effort. However, this comes at the cost of a higher abstraction level as the vessels are represented by nodes while the connections are visually encoded as edges. This does not correspond with the typical textbook illustration of the CoW. Since domain experts who are supposed to work with this visualization software are more familiar with the latter, a visualization that is inspired from the textbook illustration is more suitable than a graph. Therefore, the whole visualization approach of this thesis is based on the textbook illustration. However, since not only the shape of the CoW will be visually encoded but also up to three quantitative attributes, it is not reasonable to use a CoW illustration like the one shown in Figure 1.2 as there would not be enough space to visually encode the attributes.

3.2.1 Visualization of the different Configurations

As it was mentioned in 1.2.2, configurations that cannot be described by the classification system of Chen et al. [9] are considered as outliers. Hence, since outliers are not important when two big CoW datasets are compared, this visualization uses the classification system of Chen et al. in an extended version that covers 99.3% of the 757 findings in the two

studies [9, 16]. This assumption enables to visually encode the CoW as a shape similar to the textbook illustration. The different configurations are not displayed at once. Instead, the configurations are divided into four shapes (see Figure 3.1). This is because some configurations have vessel segments that would overlap if the shape of the configurations would be overlaid. As a result, it would not be possible to display the attributes of the overlapping segments. The user can switch between the four different shapes by scrolling the mouse wheel. Since there might be cases in which the user is only interested in the standard configuration, the latter can be visually encoded as a fifth shape.

3.2.2 Visualization of the Shape

Figure 3.2 shows the shape of a standard CoW that is visually encoded with the implemented software. The vessel segments of the CoW are visually encoded as arcs of a circle. In case of segments that are a part of the standard configuration and of the CoW, the length of the arcs based on the average length or, in case of the three main arteries (LICA, RICA, BA), on the average diameter of the vessel segments [14], i.e. segments that are larger on average are visually encoded as larger arcs. The thickness of the arcs are equal and chosen so, that the attributes have enough space to be visually encoded within the arcs. Segments that are not a part of the CoW but a part of the standard configuration, i.e. the ACA-A2 and the MCA-A1 segments, are visually encoded equal in size as arcs above the CoW segment that they branch from. Segments of non-standard configurations, e.g. the MACC in Figure 3.1, are visually encoded as arcs above their origin segment as well, whereas the size is chosen so that the different configurations fit to the screen without the need of changing the size of vessel segments that are a part of two or more configurations, e.g. the segments of the main arteries are visually encoded with the same size across all the configurations. It is of course desirable to choose the size of all arcs relative to the average size of the vessel segment that they visually encode, whether they belong to the standard CoW or not. However, to the best of our knowledge, there is no reliable data regarding the average length and diameter of all the vessel segments that are not considered as a part of the standard CoW. The segments are all labeled by a shortcut of their anatomical name.

3.2.3 Comparative Visualization of the Shapes

To be able to visually compare the average CoW of two populations, an average CoW can be visually encoded for each of the two populations. One of the average CoWs is displayed on the right of the screen and the other on the left. This enables a side-by-side comparison. Missing vessel segments are not visually encoded as a missing arc but by missing quantitative attributes (see Figure 3.3). This is because missing arcs could change the shape so, that it does not look like the typical textbook illustration shape anymore.

The segments are divided into a left and right anterior part, a posterior part and a communicating part. Each of this parts is visually encoded by a different hue. The colors are chosen from ColorBrewer [13].

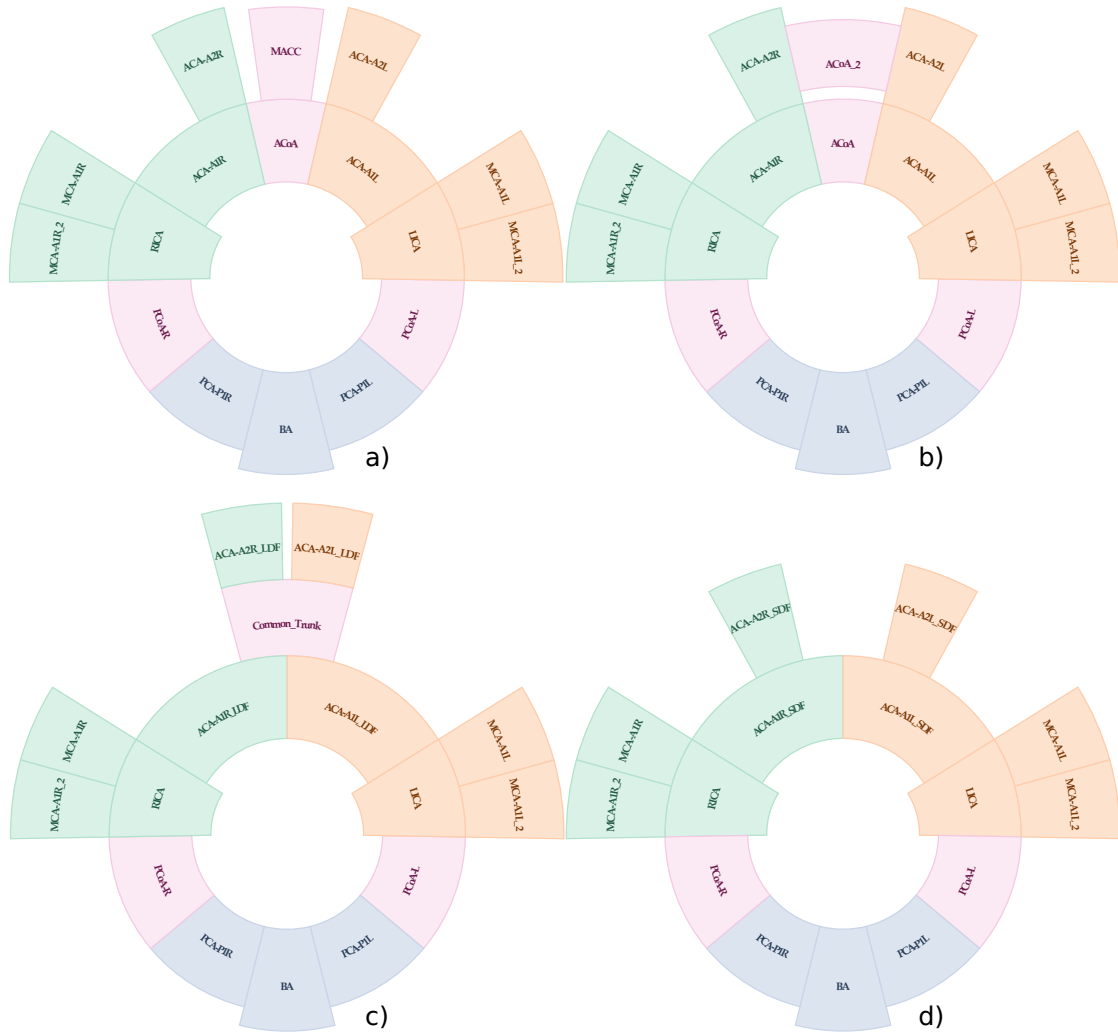


Figure 3.1 – Visualization of the four non-standard CoW configurations. As it can be seen, it is not possible to merge these configurations as some vessel segments of the anterior part would overlap. These configurations based on the classification system of Chen et al. [9]. In a) an additional medial artery of the corpus callosum (MACC) branches from the ACoA. Configuration b) shows an additional ACoA segment. In c) the left and the right ACA forms a common trunk that branches into two segments. In some cases the left and the right ACA can merge over a short distance and then branch into two segments as it is shown in d). An additional left and right MCA-A1 segment is visually encoded in all of the four configurations.



Figure 3.2 – Visualization of the standard CoW shape. Each vessel segment is visually encoded as an arc of a circle. Green segments belong to the right anterior part, orange segments to the left anterior part, blue segments to the posterior part and pink segments to the communicating part. The segments are all labeled by a shortcut of their anatomical name.

3.3 Visualization of the Quantitative Attributes

Most studies regarding the CoW are interested in the diameter of the vessel segments or in the amount of occurrence of the vessel segments within a population or in both. But there are also studies that are interested in other quantitative attributes such as the length of the vessel segments or the intensity values of the segments in MRA images. Since studies that are interested in more than three quantitative attributes are rare and visually encoding more than three quantitative attributes at once would lead to a rather complex visualization, the visualization approach in thesis is limited to three



Figure 3.3 – Visualization of the standard CoW shape with missing vessel segments. The bars visually encode quantitative attributes of the vessel segments (see Section 3.3). A vessel segment that is missing in all the subjects of a dataset has no quantitative attributes. Thus, missing bars in a vessel segment visually encode the absent of this segment. In this Figure both MCA-A1 segments, the ACoA segment and the left PCoA segment are missing.

quantitative attributes. A limitation of the attributes does not only reduce the complexity of the visualization, but it also leads to more available space for the visually encoded attributes and thus enables to visually redundancy encoding the attributes to simplify the visualization so that the viewer can see certain information quicker (see Figure 3.7). For the sake of simplicity, this thesis takes only the three attributes length, diameter and what will be referred to as "number of segments" into account. However, each of the three attributes can be replaced by any arbitrary quantitative attribute without changing the concept of this thesis' visualization approach.

The viewer should be able to see the information he is interested in with as little mental effort as possible. For this reason, the attributes are visually redundancy encoded with three different approaches. The first approach uses a juxtaposition design, the second an explicit encoding design and the third a superposition design. Each of these approaches will be discussed in a subsection.

3.3.1 Juxtaposition of the Quantitative Attributes

In this approach, the attributes are visually encoded as bars within the corresponding segment (see Figure 3.4). The category of the attributes, i.e. whether the attribute belongs to the diameter of the vessel segments, the length or the number of segments, is visually redundancy encoded with the two visual channels hue and position, as these are the most effective visual channels for categorical data (see Table 1.1). Bars that visually encode the diameter are green and closest to the inner radius of their segment, the bars for the length attribute are red and closest to the outer radius of their segment and the bars for the number of segments attributes are blue and between the length and the diameter bar. The redundant encoding enhances the perception of the viewer, as he has just to remember either the color or the position of an attribute to identify the category of the bar [24].



Figure 3.4 – Visualization of the quantitative segment attributes. The red bar visually encodes the length and is closest to the outer radius of the segment, the diameter is visually encoded by the green bar and is closest to the inner radius of the segment and the blue bar encodes the number of segments and is between the length and the diameter bar. The visually encoded values are calculated relative to the maximum value of the attributes. In this Figure, the length bar of the ACoA shows a value of 13.24%. This means that the ACoA has a length that reaches 13.24% of the maximum length that exists in the dataset of the two populations that are compared.

The number of segments attribute visually encodes the occurrence of the segments in the population as a relative number, e.g. in a population with 100 subjects, the number of segments has the value 98% for any given segment that is missing in two subjects. The diameter and the length values are either arithmetic means or percentile values of the respective population. Their relative value is calculated with Formula 3.1.

$$\text{relative value} = \frac{\text{absolute specific value} \times 100}{\max(\max(p_1(\text{absolute value})), \max(p_2(\text{absolute value})))} \quad (3.1)$$

In Formula 3.1 "absolute specific value" referred to the absolute diameter or the absolute length of a specific segment, e.g. the LICA segment in the first population. The first population is referred to as p_1 and the second population as p_2 . For example, if the largest diameter of the vessel segments across the two populations has the value 0.74 cm and the mean diameter or the diameter of a specific percentile of the ACoA in the second population is 0.24 cm, then the relative value of the ACoA in p_2 would be $\frac{0.24 \times 100}{0.74} = 32.43\%$. The 0.74 cm is the largest diameter in the datasets of the two populations.

The values are visually encoded as bars and thus with the visual channel "length". However, although length is an effective visual channel for quantitative data (see Table 1.1), it is difficult to distinguish small differences if the values have a wide range. This is especially true for bars with a small length. In this approach, the bars have a length of hundred pixels when they are displayed on a full HD display. Longer bars would be desirable, as it would be easier to distinguish small differences, but the display resolution is a limiting factor. This is an issue as actually big differences between two segments could barely be visible if e.g. these two segments have a value of 1% and 2% respectively, because the maximum value is considerably larger (see Figure 3.5). To tackle this issue, the bars can be scaled between the minimum and maximum value instead between zero and hundred. In the above example, each pixel is equal to 0.074 mm if the Formula 3.1 is used and if the bar has a width of 100 pixel. Assuming that the ACoA in the above example is the minimum value, each pixel would be equal to 0.05 mm if the range is scaled between the minimum and maximum value. A smaller $\frac{mm}{pixel}$ ratio is of course desirable. However, a minimum-to-maximum scale is harder to interpret and would not solve the issue but just weaken it.



Figure 3.5 – Visualization of the length attribute of two ACoA segments. The length of the left ACoA segment has a value of 1% while the right segment has a value of 2%. This means that the right segment is twice as big as the left one. However, because of the considerably larger maximum length, this big difference is barely visible.

In fact, each visualization approach has its benefits and drawbacks. While the bar visualization that is described in this subsection (see Figure 3.4) is useful for having

a quick overview of the magnitude of the values, it requires more mental effort to see small differences between the vessel segments. To maintain the benefits of a visualization approach without accepting its drawbacks, it can be useful to add a second visualization approach that visually redundancy encodes the same attributes but addressing other issues. For example, one approach can be used to show big differences and the other to show the small ones. Hence, instead of replacing the visualization approach that is described in Figure 3.4 by a visualization approach that enables the viewer to see large and small differences with little effort, additionally two other visualization approaches will be used to address the issue of enabling the viewer to see small differences with as little mental effort as possible. These visualization approaches will be described in the next two subsections.

3.3.2 Explicit Encoding of the Quantitative Attributes

One drawback of the attribute visualization approach that is shown in Figure 3.4 is that it requires mental effort from the user to see small differences. This is because the visual channel "length" is not effective if the values have a wide range. Consequently, reducing the range of the values can solve this issue. In Figure 3.5 the left ACoA has an absolute length of 0.4 cm and the right ACoA a length of 0.8 cm. But the maximum length has a value of 40 cm. As a result, the absolute values ranges from 0 to 40 cm. If, however, the two ACoAs are compared to each other independent of the values of the other segments, the absolute values would range from 0 to 0.8 cm. This approach reduces the range considerably, but at the cost of losing the relation to the other segments. Visually encoding a bar for each comparison of two segments is not suitable as that would require $\frac{(n-1)^2 \times (n-1)}{2}$ bars for each attribute, where n is the number of different segments (ACoA, RICA, LICA, ...). However, since usually the comparisons of two corresponding segments are the most interesting ones, e.g. a comparison between the ACoA of the first population with the ACoA of the second population, it is reasonable to use this or a similar approach to at least enable a quick distinction of small differences between two corresponding segments. In this thesis a similar approach is used, as visually encoding two bars of the same attribute in each segment would be confusing. The used approach is shown in Figure 3.6.

Instead of visually encoding the difference between two corresponding segments as a relative value, there are just three values that are visually encoded: an attribute value of a segment is either significantly larger or significantly smaller than the other one or approximately equal to it. This is visually encoded by the lightness and the opacity of a circle. If a segment has a significantly larger value of an attribute, then the circle of this attribute will be dark, if the value is significantly smaller, then the circle will be bright and if the values are approximately equal, then the opacity of the circle will be 0. Like the bars (see Figure 3.4), the category of a circle is redundancy encoded by the two visual channels hue and position. The values of the circles are calculated with Formula 3.2.



Figure 3.6 – Visualization of significant differences between two corresponding segments. A red circle that is closest to the outer radius visually encodes the differences of the length attribute, a green circle that is closest to the inner radius visually encodes the differences of the diameter attribute and a blue circle that is between the red and the green circle visually encodes the differences of the number of segments attribute. If an attribute value of a segment is significantly larger than the attribute value of the other segment, then the lightness of the circle will be dark, if the attribute value is significantly smaller, then the circle will be light and if the values are approximately equal, then the opacity of the circle will be 0. In this Figure, the length attribute of the left segment is significantly smaller than the length attribute of the right segment while the diameter attribute is significantly larger and the number of segments attributes are equal.

$$\text{value}(\text{segment}) = \frac{\max(\text{attr}(p_1(\text{segment})), \text{attr}(p_2(\text{segment})))}{\min(\text{attr}(p_1(\text{segment})), \text{attr}(p_2(\text{segment})))} \quad (3.2)$$

In Formula 3.2 *attr* referred to the length, diameter or number of segments attribute. The first population is referred to as p_1 and the second population as p_2 . For example, if the length of the ACoA in the first population is 0.7 cm and the length of the ACoA in the second population 0.5 cm, then $\text{value}(\text{ACoA})$ would be $\frac{0.7}{0.5} = 1.4$. That means that the bigger ACoA is 40% larger than the smaller one. A circle is only visible, if $\text{value}(\text{segment})$ has a value greater than or equal to 1.3. This approach enables to see small differences between the two corresponding segments immediately while keeping the visualization simple.

The value of 1.3 was chosen arbitrary to demonstrate the concept of this approach. The idea of this approach is that the viewer is not primarily interested in the exact value of the difference, but whether there is a significant difference or not. Existing circles indicates that there is a significant difference while missing circles tells the viewer immediately that there is not a significant difference between the two corresponding segments. This approach assumes that only if there is a significant difference, the viewer will be interested in the exact difference. Figure 3.7 shows a visualization of the standard CoW with the implemented attribute visualization approaches that are described in Figure 3.4 and Figure 3.6.



Figure 3.7 – Visualization of the standard CoW with the implemented attribute visualization approaches that are described in Figure 3.4 and Figure 3.6

3.3.3 Superposition of the Quantitative Attributes

If the viewer wants to compare the attributes of two segments, a side-by-side comparison would require more mental effort than a superposition comparison. This is because in a side-by-side comparison the viewer has to memorize the appearance of the objects to be able to compare them. In fact, a side-by-side comparison of the bars enforces the viewer to mentally do a superposition comparison. Furthermore, it is easier to distinguish small differences with a superposition design. Therefore, an attribute visualization approach that uses a superposition design is preferable. However, since it is not reasonable to overlay the bars of all segments, a superposition design that requires user interaction will be used additionally to the juxtaposition approach instead of replacing it. Figure 3.8 shows the used superposition design. In this approach, the user can click on a segment

to highlight it and overlay its attribute values over the attribute values of all the other segments. The highlighting enables the viewer to see to which segment the overlaid values belong without to memorize on which segment he has clicked.

The color of the overlaid bars is a high saturated yellow. There are two reason for this color decision. First, it is assumed that a viewer who clicks on a segment to overlay its attributes over the attributes of the other segments is primarily interested in the difference between the overlaid attributes of the segment he has clicked on and the attributes of the other segments. A proper visualization should help the viewer to focus on this comparison. This is achieved by the popup effect of the high saturated yellow. The second reason is that the color contrast between the bars of the segments and the overlaid bars has to be high to be able to see the overlaid bars with little effort.

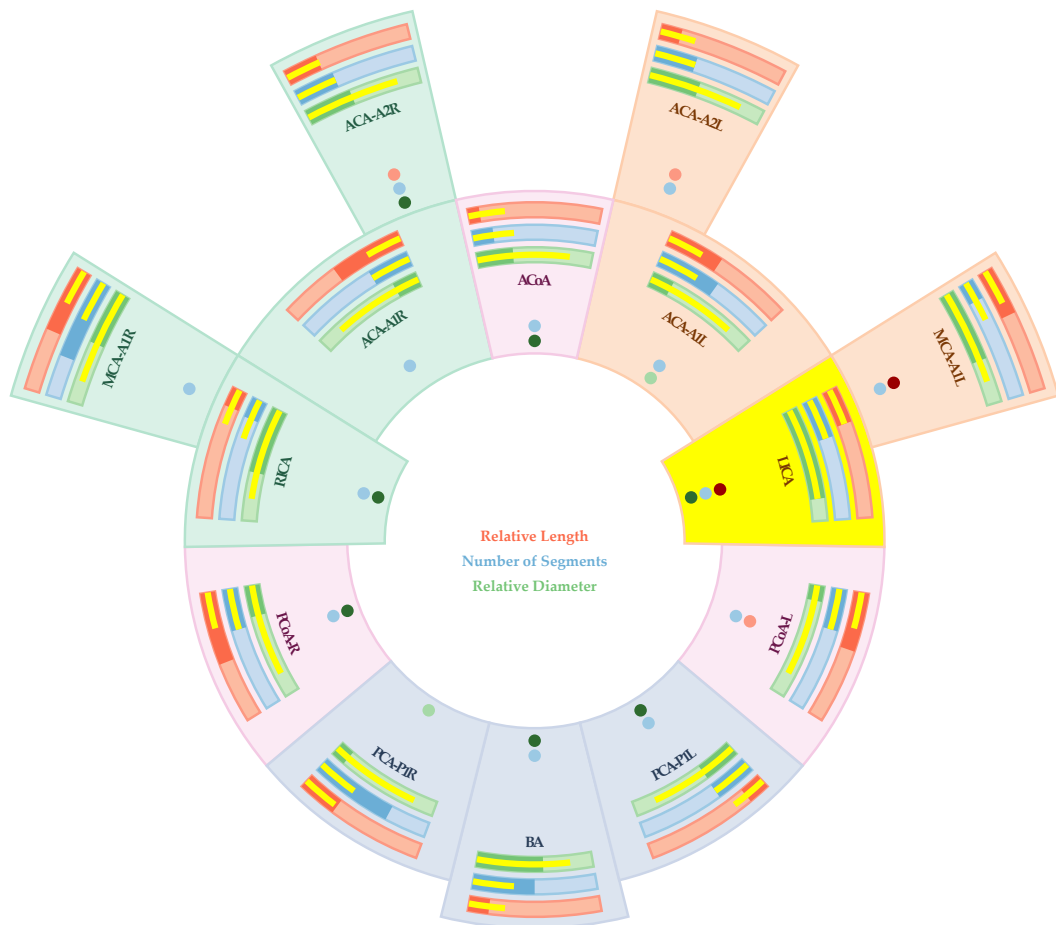


Figure 3.8 – Superposition of the quantitative attributes. The overlaid yellow bars visually encode the attribute values of the LICA. Additionally, the LICA is highlighted with the same color as the bars to enable the user to see which segments the yellow bars belong to.

3.4 Data Acquisition

It would be ideal if the implementation acquires the data directly from the images of the medical imaging devices. However, algorithms that enables a reliable anatomical labeling of the segments are not a part of this thesis. There is a promising approach from Bogunovic et al. [5] that classifies the segments based on a maximum a posterior probability. A similar algorithm can be implemented as a future work either to completely automate the data acquisition or to support it. In this thesis, the implementation uses a XML file for each CoW (see Listing 1).

Listing 1 – Example of the XML structure of the input data.

```
<!DOCTYPE AVPvesseltree>
<vesseltree>
  <segment id="1">
    <description>BA</description>
    <length>0.58</length>
    <diameter>0.68</diameter>
  </segment>
  <segment id="2">
    <description>LICA</description>
    <length>0.56</length>
    <diameter>0.18</diameter>
  </segment>
  <segment id="3">
    <description>PCA-P1R</description>
    <length>1.26</length>
    <diameter>0.083</diameter>
  </segment>
</vesseltree>
```

The file contains a description of the segments and the attributes of the segments. Since data acquisition is not automated, it is crucial to enable the creation of the input data with as little effort as possible. For this reason, the connections between the segments are not explicitly coded in the XML file. Instead, it is assumed that the segments are always connected like the segments in the standard CoW or the other supported configurations. For example, it is assumed that the BA is connected to the right PCA if the latter exists in the XML file, as the BA is connected with the right PCA in all configurations. Figure 3.9 shows the visualization of the XML file in Listing 1.

Table 3.1 shows all labels of the supported segments. The term "sdf" refers to the fusion of the both ACAs over a short distance (thus "short distance fusion") and "ldf" to the fusion of the both ACAs over a long distance. "common_trunk" refers to the segment that is formed by the fusion of the both ACAs in the ldf configuration (see Figure 3.1). As all supported configurations can be described with this XML structure, there is no need to require an explicit coding of the connections.

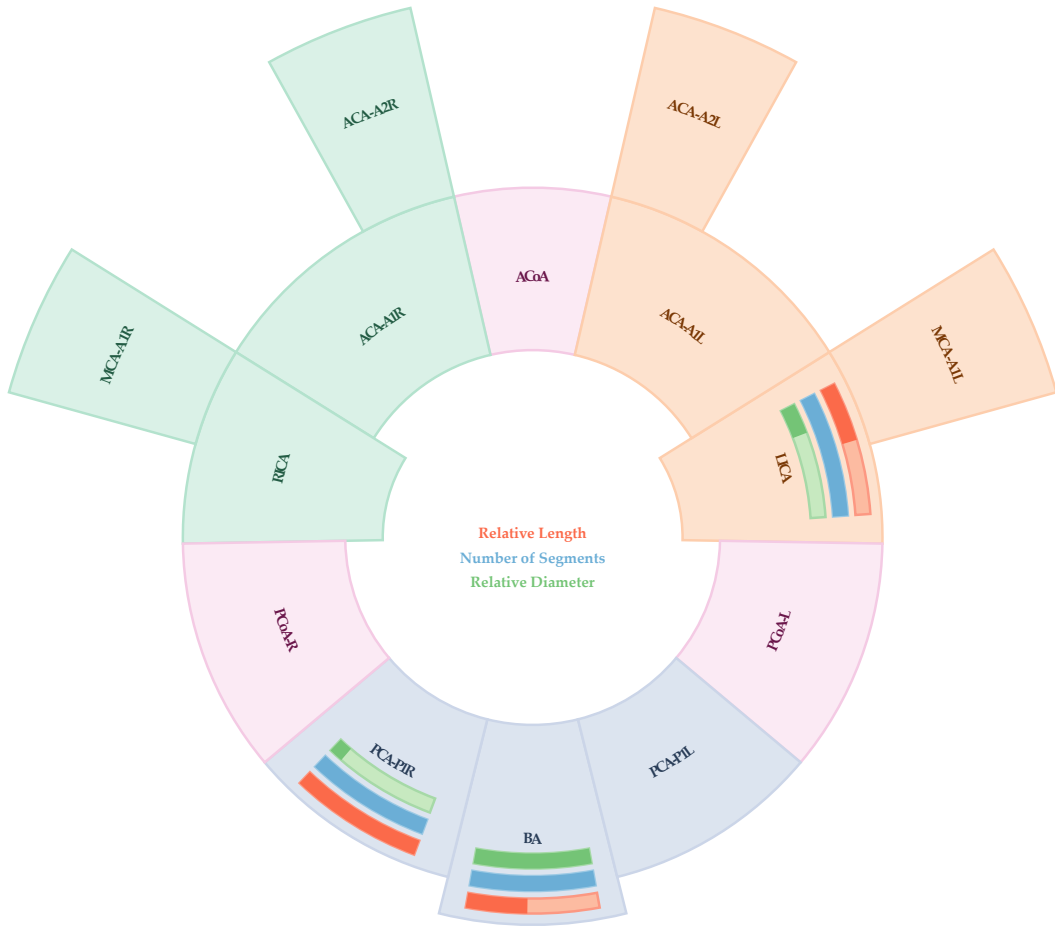


Figure 3.9 – Visualization of the XML file that is shown in Listing 1.

Left Anterior	Right Anterior	Posterior	Communicating
lica	rica	ba	acoa
aca-a1l	aca-a1r	pca-p1l	pcoa-l
aca-a1l_sdf	aca-a1r_sdf	pca-p1r	pcoa-r
aca-a1l_ldf	aca-a1r_ldf		macc
aca-a2l	aca-a2r		common_trunk
aca-a2l_sdf	aca-a2r_sdf		
aca-a2l_ldf	aca-a2r_ldf		
mca-a1l	mca-a1r		
mca-a1l_2	mca-a1r		

Table 3.1 – All labels of the supported segments.

3.5 User Interaction

While the user interaction can be arbitrarily complex, a proper visualization should reduce the interaction to a minimum and in exchange show as many information as possible without the need of user interaction. In this thesis, the user interaction is reduced to five options. First, it was chosen to not show all configurations at once. Instead, the user can scroll with the mouse wheel to choose between possible configurations. The reason for this decision is that it is not possible to visually encode all the configurations at once while retaining the shape of the typical textbook illustration as some segments would overlap. Furthermore, the user may be interested in comparing the configurations of the two populations individually, e.g. the standard configuration of p_1 with the standard configuration of p_2 . In cases like this example, it is helpful to hide segments that do not belong to the configuration. The second option is the possibility to hide attributes by clicking on a checkbox (see Figure 3.10). This is because the user may be interested in just one or two attributes. Of course, the user can also simply not code a third or a second attribute in the XML files. However, the possibility of hiding attributes increases the flexibility as the user can use one XML file for different tasks. As a third option, the user can choose whether the mean of the population's attributes is shown, which is the default, or a specific percentile (5th, 25th, 50th, 75th or 95th) as the user may be interested in comparing the distribution of the populations or a patient's CoW with different percentiles of a population. There are of course much more statistical information that can be calculated by the visualization software, e.g. whether the differences have a statistical significance. But since this thesis focuses on the visualization, such statistic calculations are not implemented. The fourth option is the possibility to overlay bars of a segment over all bars of the other segments by clicking on the segment (see Figure 3.8). If the user holds the mouse over a segment, the numerical values of its attributes will be displayed at the center of the CoW (see 3.11). This is the fifth option. Figure 3.11 shows the user interface of the implementation.

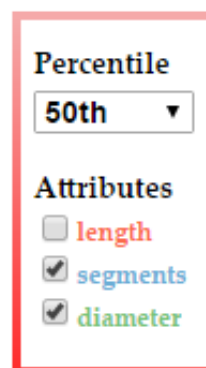


Figure 3.10 – Preferences box of the implementation. The selection enables to choose between the percentiles (5th, 25th, 50th, 75th or 95th) or the arithmetic mean, which is the default. With the checkboxes the user can hide the attributes.

Future Work and Discussion

In this thesis, a comparative visualization software was implemented that enables to visually encode the CoWs of a population as an average CoW and to compare it with another average CoW or with the CoW of a single subject. The objective was a visualization that is as intuitive as possible. For this reason, the whole approach was inspired from the typical textbook illustration of the CoW. However, this approach is a trade-off as it is not as scalable as others, such as a graph visualization. As a result, the used approach is limited to the configurations of the classification system of Chen et al. [9] (see Figure 1.3). Although this classification system covers the most common configurations, in some cases it is desirable to be also able to visually encode other possible configurations, which this thesis' approach considers as outliers. Hence, as a future work, this thesis' approach can be extended to visually encode all theoretically possible configurations while retaining a shape similar to the typical textbook illustration. A further limitation of this thesis' approach is that the configurations cannot be shown at once. Instead, the user has to scroll the mouse wheel to choose between the different configurations (see Figure 3.1). This works well, if the user can only switch between a few configurations. However, if a half dozen or more configurations are supported then an alternative to the mouse wheel approach should be used. For example, instead of scrolling the mouse wheel to choose a configuration, an approach similar to the one used in Cerebral (see Section 2.1.1) can be implemented that shows all the configurations in low detail and visually encodes a configuration in more detail if the user clicks on it. A third limitation is that it is not possible to compare more than two average CoWs at once. This decision was primarily made due to the limited display size. As a future work, the visualization design can be improved to at least enable a comparison between three average CoWs at once as in some studies there are more than two average CoWs that are compared (see [10] for an example).

Since this thesis focuses on the visualization of the CoW, data acquisition was not an issue. However, an automated data acquisition from medical imaging devices is from high

interest, as acquiring the data manually requires a tremendous amount of effort. Miao et al. [20] developed a visualization software that acquires the data automatically, but to be able to do so, they used a labeling system from which the anatomical name of the segments cannot be safely concluded, though experienced radiologists can assume which label describes which segment. Bogunovic et al. [5] propose an approach that is able to label the most important segments of the CoW with a high reliability. An algorithm that is based on this approach can be implemented to enable a faster data acquisition.

Although the topic of this thesis was an idea of a radiologist, the implemented software was not evaluated by a domain expert. This can be done as a future work. Since this software has the potential to enhance the physician-patient consultation as the visualization is easy to understand, an evaluation by some non-professionals, i.e. potential patients, is also desirable.

List of Figures

1.1	MRA slice of the brain's vessels	2
1.2	Nomenclature of the basal cerebral arteries of the CoW	3
1.3	Schematic diagrams of anatomic variations of the Circle of Willis	5
1.4	Ten unclassified variants of the anterior part of the Circle of Willis	5
1.5	Visualization of a number sequence	7
2.1	Cerebral	11
2.2	StemView	13
2.3	Circle of Willis Radar	14
3.1	Visualization of the four non-standard Circle of Willis configurations	20
3.2	Visualization of the Circle of Willis shape	21
3.3	Visualization of the Circle of Willis shape with missing vessel segments	22
3.4	Visualization of the quantitative segment attributes	23
3.5	Visualization of the length attribute of two ACoA segments	24
3.6	Visualization of significant differences between two corresponding segments	26
3.7	Visualization of the standard Circle of Willis	27
3.8	Superposition of the quantitative attributes	28
3.9	Visualization of the XML file that is shown in Listing 1	30
3.10	Preferences box of the implementation	31
3.11	User interface of the implementation	32

List of Tables

1.1	Effectiveness of visual channels depending on the attribute type [21].	8
-----	--	---

3.1	All labels of the supported segments.	30
-----	---	----

Bibliography

- [1] The top 10 causes of death, 2014. URL <http://www.who.int/mediacentre/factsheets/fs310/en/>. [Online; accessed 07-September-2016].
- [2] Nomenclature of the basal cerebral arteries of the circle of willis, 2016. URL <http://radiologykey.com>. [Online; accessed 07-September-2016].
- [3] A. Barsky, T. Munzner, J. Gardy, and R. Kincaid. Cerebral: Visualizing multiple experimental conditions on a graph with biological context. *IEEE Computer Society*, 14(6):1253–1260, 2008.
- [4] T. Beach, J. Wilson, L. Sue, A. Newell, M. Poston, R. Cisneros, Y. Pandya, C. Esh, D. Connor, M. Sabbagh, D. Walker, and A. Roher. Circle of willis atherosclerosis: association with alzheimer’s disease, neuritic plaques and neurofibrillary tangles. *Acta Neuropathologica*, 113:13–21, 2007.
- [5] H. Bogunovic, J. Pozo, R. Cardenes, S. R. L, and A. Frangi. Anatomical labeling of the circle of willis using maximum a posteriori probability estimation. *IEEE Transactions on medical imaging*, 32(9):1587–1599, 2013.
- [6] M. Bostock, V. Ogievetsky, and J. Heer. Data-driven documents. *IEEE Transactions on Visualization and Computer Graphics*, 17(12):2301–2309, 2011.
- [7] A. Bouthillier, H. van Loveren, and J. T. Keller. Segments of the internal carotid artery: A new classification. *Neurosurgery*, 38:425–433, 1996.
- [8] H. Brkic, S. Mrdenovic, R. Radic, and G. Curic. Function of circle of willis. *Journal of Cerebral Blood Flow and Metabolism*, 34:578–584, 2014.
- [9] H.-W. Chen, P.-S. Yeb, C.-C. Lee, C.-C. Chen, P.-Y. Chang, S.-K. Lee, W.-H. Lee, C.-M. Ling, and A. S.-B. Chau. Magnetic resonance angiographic evaluation of circle of willis in general population: A morphologic study in 507 cases. *Chinese Journal of Radiology*, 29:223–229, 2004.
- [10] B. Cucchiara, R. Wolf, L. Nagae, Q. Zhang, S. Kasner, R. Datta, G. Aguirre, and J. Detre. Migraine with aura is associated with an incomplete circle of willis: Results of a prospective observational study. *PLOS ONE*, 8(7):e71007, 2013.

- [11] M. Gleicher, D. Albers, R. Walker, I. Jusufi, C. D. Hansen, and J. C. Roberts. Visual comparison for information visualization. *SAGE Publications*, 10(4):289–309, 2011.
- [12] J. Guerra-Gomez, M. Pack, C. Plaisant, and S. B. Visualizing change over time using dynamic hierarchies: Treeversity2 and the stemview. *IEEE Transactions on Visualization and Computer Graphics*, 19(12):2566–2575, 2013.
- [13] M. Harrower and C. A. Brewer. Colorbrewer.org: An online tool for selecting colour schemes for maps. *The Cartographic Journal*, 40(1):27–37, 2003.
- [14] S. Kamath. Observations on the length and diameter of vessels forming the circle of willis. *Journal of Anatomy*, 133:419–423, 1981.
- [15] K. Kapoor, B. Singh, and D. L. Inder. Variations in the configuration of the circle of willis. *Anatomical Science International*, 83:96–106, 2008.
- [16] W. Klimek-Piotrowska, M. Kopec, M. Kochana, R. Krzyzewski, K. Tomaszewski, P. Brzegowy, and J. Walocha. Configurations of the circle of willis: a computed tomography angiography based study on a polish population. *Folia Morphologica*, 72:293–299, 2013.
- [17] J. Kurskal and J. Landwehr. Icicle plots: Better displays for hierarchical clustering. *Taylor and Francis*, 37(2):162–168, 1983.
- [18] M. M. Malik, C. Heinzl, and M. E. Gröller. Comparative visualization for parameter studies of dataset series. *IEEE Transactions on Visualization and Computer Graphics*, 16(5):829–840, 2010.
- [19] M. Meyer, T. Munzner, and H. Pfister. Mizbee: A multiscale synten browser. *IEEE Transactions on Visualization and Computer Graphics*, 15(6):897–904, 2009.
- [20] H. Miao, G. Mistelbauer, C. Našel, and M. E. Gröller. CoWRadar: Visual quantification of the circle of willis in stroke patients. In K. Bühler, L. Linsen, and N. W. John, editors, *EG Workshop on Visual Computing for Biology and Medicine*, pages 1–10. The Eurographics Association, 2015.
- [21] T. Munzner. Visualization. In P. Shirley and S. Marschner, editors, *Fundamentals of Graphics, Third Edition*, chapter 27, pages 675–707. Taylor and Francis, 2009.
- [22] K. Parsaye and M. Chignell. *Intelligent Database Tools and Applications: Hyperinformation Access, Data Quality, Visualization, Automatic Discovery*. John Wiley & Sons, Inc., New York, NY, USA, 1st edition, 1993. ISBN 0471570656.
- [23] T. van Seeters, J. Hendrikse, G. Biessels, B. Velthuis, W. Mali, L. Kappelle, and Y. van der Graaf. Completeness of the circle of willis and risk of ischemic stroke in patients without cerebrovascular disease. *Neuroradiology*, 57:1247–1251, 2015.
- [24] C. Ware. Visual salience and finding information. In C. Ware, editor, *Information Visualization*, chapter 5, pages 139–177. Elsevier, 2012.